IEEE ComSoc IEEE Open Journal of the Communications Society

Received 29 October 2023; revised 13 December 2023; accepted 30 December 2023. Date of publication 2 January 2024; date of current version 22 January 2024.

Digital Object Identifier 10.1109/OJCOMS.2023.3349277

Uplink Data Rate Maximization in Multi-Cell BackCom NOMA Systems

DINGJIA LIN (Student Member, IEEE), KAIDI WANG (Member, IEEE), TIANQI WANG, AND ZHIGUO DING (Fellow, IEEE)

School of Electrical and Electronic Engineering, University of Manchester, M1 3BB Manchester, U.K.

CORRESPONDING AUTHOR: D. LIN (e-mail: dingjia.lin@postgrad.manchester.ac.uk)

This work was supported in part by the U.K. EPSRC under Grant EP/W034522/1, and in part by H2020 H2020-MSCA-RISE-2020 under Grant 101006411.

ABSTRACT This paper investigates a backscatter communication (BackCom) non-orthogonal multiple access (NOMA) system with numerous base stations (BSs) and backscatter devices (BDs). The objective is to maximize sum uplink rate by adjusting reflection coefficients of BDs and establishing association policies between BSs and BDs. To achieve this, matching theory is utilized to address the association problem, and a quadratic transform iterative algorithm is employed to calculate optimal reflection coefficients under a given association policy. Meanwhile, hybrid successive interference cancellation (SIC) is applied to reduce the outage probability of the proposed system while optimizing the uplink sum data rate, where a low-complexity solution is developed. Simulation results validate the superiority of the proposed optimization scheme in enhancing uplink sum data rate. The comparison between BackCom NOMA and BackCom orthogonal multiple access (OMA) reveals superior performance of the former, which becomes increasingly evident as the number of BSs and BDs increases. The proposed iterative algorithm significantly enhances the system's sum uplink data rate. The usage of hybrid SIC also notably declines the outage probability of the system.

INDEX TERMS Backscatter communication (BackCom), hybrid successive interference cancellation (SIC), non-orthogonal multiple access (NOMA), resource allocation, user association.

I. INTRODUCTION

BACKSCATTER communication (BackCom) has gained notable traction in Internet of things (IoT) device applications, largely attributed to its intrinsic energy efficiency [1]. This efficiency arises from the device's non-reliance on generating its radio waves, significantly reducing power consumption [2]. Simultaneously, the typical utilization of BackCom devices basic hardware results in a cost-effective manufacturing approach [3]. The ease of integrating BackCom into current wireless apparatus, circumventing the need for intricate transmitters, underscores its simple integration benefits [4]. In addition, its operation devoid of radio wave emissions reflects an environmentally-friendly aspect by minimizing electromagnetic radiation impacts [5]. Meanwhile, non-orthogonal multiple access (NOMA) is spotlighted as a crucial innovation technique to define future wireless communication systems [6], [7], [8], [9], [10]. Its prowess lies in elevating the spectral efficiency of the system [11]. A pivotal strength of NOMA is its potential to accommodate a plethora of device connections, especially marking its relevance for extensive IoT applications [12]. Contrasted with traditional orthogonal multiple access (OMA) technologies, NOMA can enhance overall throughput of the system [13]. Both BackCom and NOMA possess distinct advantages in their domains, and the amalgamation of these two technologies can unlock specific synergistic benefits and bolstered functionalities. Such a fusion can augment the spectral efficiency, pave the way for extensive low-energy communication deployments, and assure a more comprehensive and deeper network coverage while accommodating a vast array of devices [14].

A. RELATED WORKS

References [4], [15], [16], [17], [18], [19], [20] focus on the application of optimization algorithms to different system models of BackCom NOMA. As revealed in [4], ambient

BackCom confronts the issue where a single device might inadvertently utilize multiple orthogonal resource blocks, thereby compromising spectral efficiency and connectivity. The letter also underscores that NOMA can enhance throughput and support extensive connectivity in ambient BackCom networks, where two transceiver design strategies are introduced to balance system performance against complexity. Reference [15] considers a single-cell model with one downlink user and multiple backscatter devices (BDs), in which the average uplink sum data rate is maximized by adjusting reflection coefficients. Transformation of the initial fractional problem into a linear format aids in determining optimal reflection coefficients, the uplink sum data rate of the BackCom NOMA system improves, which performs better than the BackCom OMA system. Further research in [16] and [17] explores a multi-antenna BackCom NOMA system. In [16], beamforming vectors adjustment is utilized to optimize uplink rate, with semidefinite relaxation (SDR) facilitating problem transformation and Gaussian randomization enabling optimal beamforming matrix derivation. Reference [17] maximizes energy efficiency using BD reflection coefficients and beamforming vectors adjustments, with the Dinkelbach algorithm managing the fractional format of the objective function and penalty SDR obtaining the optimal beamforming matrix. In [18], cognitive radio (CR) and BackCom NOMA are combined to bolster spectrum and energy efficiency in future IoT systems. The paper introduces a robust resource allocation approach for NOMA in cognitive BackCom networks, addressing the challenges of channel estimation errors and catering to a massive number of IoT nodes. The optimization problem aims to maximize total throughput by fine-tuning transmission parameters, and an iterative algorithm is proposed for its solution. Simulations suggest the algorithm's superiority in terms of throughput and robustness when compared to benchmark algorithms. In [19], the integration of wireless-powered communication with BackCom is presented as an ideal model for future IoT systems. The study delves into a robust resource allocation challenge for such systems, emphasizing the impact of real-world channel uncertainties and nonlinear energy harvesting models. By optimizing various system parameters, including the beamforming vector and transmit power, a novel algorithm is proposed, showing notable improvements in system robustness against benchmarks. Further research might explore Gaussian channel state information (CSI) errors given accessible CSI estimation error models. The study in [20] explores the performance of a monostatic BackCom system employing hybrid time-division multiple-access/power-domain NOMA, addressing both static and dynamic frameworks. For the static framework, two novel schemes, namely two-node pairing and adaptive power reflection coefficient, are introduced to elevate performance over conventional systems. Transitioning to the dynamic framework, two additional methods, dynamic-sized pairing and hybrid adaptive power reflection coefficient/dynamic-sized pairing, are proposed. Performance metrics indicate the proposed methods' superiority over conventional approaches, with potential future investigations into imperfect CSI and system optimization. Reference [21] optimized beamforming in a symbiotic radio network with a primary user and a secondary backscatter network, employing techniques including alternative optimization and semi-definite relaxation to tackle non-convex resource allocation challenges, achieving notable performance gains. Reference [22] presents a hybrid BackCom and wireless powered NOMA network for IoT, employing a two-layer iterative algorithm to optimize throughput fairness among IoT devices. The methodology transforms a non-convex problem to a convex one, improving energy and data transmission efficiency. Simulations confirm the proposed model's superiority in achieving max-min throughput compared to existing approaches.

B. MOTIVATION AND CONTRIBUTIONS

The combination of BackCom and NOMA technologies markedly improves spectral efficiency, a crucial aspect in scenarios with limited spectrum resources. BackCom systems are known for their low energy consumption, making them ideal for IoT devices and sensor networks, especially in environments where resources are constrained. In the realm of current wireless communication research, exploring BackCom NOMA systems in multi-cell contexts is a relatively new area. These scenarios differ from BackCom OMA systems in that they require the management of both intra- and inter-cell interference, adding layers of complexity to the optimization process. In such environments, modifications in the state of any BDs, including changes in user associations or resource allocations, impact both types of interference, thereby affecting all users within the network. Additionally, the adoption of hybrid successive interference cancellation (SIC) in BackCom NOMA systems has not been extensively explored, offering opportunities for further studies. Research has shown that using hybrid SIC in uplink networks based on NOMA can lead to enhanced performance [23], [24]. The feature of hybrid SIC to flexibly adjust the decoding sequence of BDs helps in maintaining data rates and minimizing error floors, constrained only by user data rates [25], [26]. Implementing hybrid SIC allows for a dynamic adjustment in decoding order, thereby increasing the likelihood of BDs meeting their targeted uplink QoS.

The main contributions of this work are presented as follows:

- This work introduces an innovative multi-base station (BS) BackCom NOMA model, incorporating an multiple BSs, BDs, and user equipments (UEs). It uniquely encompasses both inter- and intra-cell interference, a concept previously unexplored. The use of power-independent BDs elevates the uplink data rate, while the deployment of multiple BSs expands network coverage, thereby augmenting both network capacity and energy efficiency.

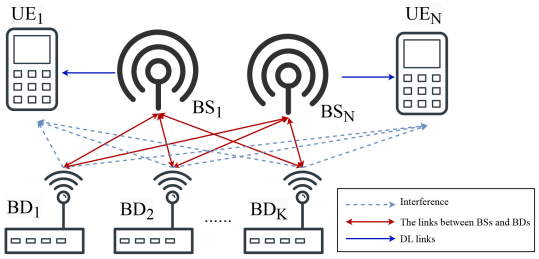

FIGURE 1. The system model of *N* BSs, *N* UEs and *K* BDs.

- The study focuses on optimizing the uplink sum data rate by fine-tuning reflection indices and the association scheme between BSs and BDs. Addressing the association challenge is accomplished through the application of matching theory, whereas the resource allocation problem, characterized by a sum of ratio forms in the objective function, is tackled using a quadratic transform algorithm. Comprehensive analysis covering complexity, convergence, and stability of the proposed solution is also presented.
- The research takes into account the downlink QoS constraints and varying BD-to-BS target uplink rates, reflecting more realistic operational scenarios. To mitigate outage probability errors, hybrid SIC is utilized, confirming that the decoding order does not affect the uplink sum data rate.
- Comparative simulation results reveal the enhanced performance of BackCom NOMA over BackCom OMA. Notably, the system's performance improves with an increased count of BDs or BSs. Conversely, an upsurge in the self-interference coefficient or target downlink data rate adversely affects performance. The implementation of hybrid SIC theory effectively reduces the outage probability in the BackCom NOMA system.

The structure of this paper is outlined as follows. Section II introduces the BackCom NOMA system model under consideration. Section III formulates the optimization problem aimed at maximizing the uplink sum data rate. Section IV discusses the application of matching theory to derive the optimal association scheme and the quadratic transform is employed to devise the optimal resource allocation strategy, including the discussion on hybrid SIC decoding order. Sections V and VI are dedicated to presenting the simulation results and drawing conclusions, respectively.

II. SYSTEM MODEL

Fig. 1 illustrates the system model of N BSs and K BDs. Consider a BackCom NOMA system with N full duplex BSs, N UEs, and K BDs, each BS communicates with a single UE and the number of BDs is greater than or equal to the number of BSs,[1] i.e., $K \geq N$. All of the BSs, UEs and BDs are equipped with a single antenna. In the considered system, the UEs and BDs can be respectively regarded as the primary users and the secondary users in a CR system. All BSs share the transmitted symbols and there are no links between BSs. And the UEs cannot decode the signals from BDs. BS_n broadcasts the symbol $s_{n,0} \in \mathbb{C}$ to all BDs and UEs and the transmission power is given by P_0. The signal reflected by BDs is denoted by $s_k \in \mathbb{C}$, $k = 1, \ldots, K$, which can be regarded as the interference at the UEs. The signals reflected by associated BDs can be decoded by the corresponding BS_n and the signals from the unassociated BDs is viewed as inter-cell interference. In this scenario, each UE is connected to one BS. Due to the other UEs are far away from BS_n, the other UEs cannot receive the signals from BS_n. The terms $h_{n,k} \in \mathbb{C}$, $h_{n,0} \in \mathbb{C}$ and $g_{n,k} \in \mathbb{C}$ refer to the channels between BD_k and BS_n, BS_n and BS_n, and BD_k and UE_n. By introducing the associate coefficient $\mathbf{X} \in \mathbb{R}^{N \times K}$ and $x_{n,k} \in \{0, 1\}$, i.e., if BS_n is associated with BD_k, $x_{n,k} = 1$, otherwise, $x_{n,k} = 0$, the reflected signal from BD_k is expressed by

$$\chi_k = \sqrt{P_0}\sqrt{\eta_k} s_k \sum_{n=1}^{N} h_{n,k} s_{n,0}, \tag{1}$$

where η_k denotes the reflection index of BD_k. The uplink signal received at BS_n is given by

$$y_n = \sum_{i=1}^{K} x_{n,i} h_{n,i} \chi_i + \sum_{j=1}^{K} \big(1 - x_{n,j}\big) h_{n,j} \chi_j + s_{\text{SI},n} + n_{\text{BS},n}, \tag{2}$$

where $s_{\text{SI},n} \sim \mathcal{CN}(0, \alpha P_0 |h_{\text{SI},n}|^2)$ is the self-interference at BS_n, α is self-interference coefficient and $h_{\text{SI},n} \in \mathbb{C}$ denotes to self-interference channel coefficient for BS_n, $n_{\text{UE},n}$ is the received noise at UE_n. Due to all the UEs can received the interference reflected by all BDs. The signal received by UE_n is expressed by

$$y_{\text{UE}_n} = \sqrt{P_0} h_{n,0} s_{n,0} + \sum_{i=1}^{K} \sqrt{\eta_i} g_{n,i} y_{\text{BD}_i} s_i + n_{\text{UE},n}, \tag{3}$$

where the noise power, both $n_{\text{BS},n}$ and $n_{\text{UE},n}$ are equal to σ^2.

A. APPLICATION OF HYBRID SIC

Assume all of the BSs can perfectly decode the signals from all associated BDs, in other words, SIC is carried out perfectly in this uplink NOMA system. The uplink signal reflected by BDs and received at their associated BS can be regarded as the conventional uplink NOMA model [27], indicating that the uplink sum data rate performance will not be influenced with the given user association and resource allocation. In this case, hybrid SIC is adopted to improve the outage probabilities of BDs. When BS_n receives the signal from BD_k, SIC is implemented with the decoding order $\mathcal{Q}$, where $\mathbf{Q}_n$ denotes the mapping from the BS_n to its decoding order and $\mathcal{Q} = [\mathbf{Q}_1, \ldots, \mathbf{Q}_N]$, which present the different

1. Please note that the case $K < N$ is simpler than the considered scenario as it can be treated as a BackCom OMA system without intra-cell interference. The solution proposed in this work can also be utilized to solve a problem in this case.

uplink data rate when $\mathcal{Q}$ varies. When decoding the signals from BD_k, the decoding order which is $[\mathrm{BD}_1, \ldots, \mathrm{BD}_K]$, and the intra-cell interference is given by

$$I_{\mathrm{Intra},n}^{(\mathbf{Q}_n)}(k) = \sum_{i=k+1}^{K} x_{n,i}\eta_i P_{\mathrm{BD}_i}\left|h_{n,i}\right|^2, \tag{4}$$

where P_{BD_k} denotes the power of the signal received by BD_k which is given by

$$P_{\mathrm{BD}_k} = P_0 \sum_{n=1}^{N}\left|h_{n,k}\right|^2\left|s_{n,0}\right|^2. \tag{5}$$

The downlink data rate at UE_n can be expressed as follows

$$R_n = \log_2\left(1 + \frac{P_0\left|h_{n,0}\right|^2}{\sum_{i=1}^{K}\eta_i P_{\mathrm{BD}_i}\left|g_{n,i}\right|^2 + \sigma^2}\right). \tag{6}$$

The uplink data rate from BD_k to BS_n is

$$R_{n,k}^{(\mathbf{Q}_n)} = \log_2\left(1 + \frac{\eta_k P_{\mathrm{BD}_k}\left|h_{n,k}\right|^2}{I_{\mathrm{Intra},n}^{(\mathbf{Q}_n)}(k) + I_{\mathrm{Inter}}(n) + \delta_n}\right), \tag{7}$$

where $\delta_n = \alpha P_0|h_{\mathrm{SI},n}|^2 + \sigma^2$, $I_{\mathrm{Inter}}(n)$ represents the inter-cell interference for BS_n and BD_n which is given by

$$I_{\mathrm{Inter}}(n) = \sum_{j=1}^{K}\left(1 - x_{n,j}\right)\eta_j P_{\mathrm{BD}_j}\left|h_{n,j}\right|^2. \tag{8}$$

Specifically, when $\mathrm{BD}_{k'}$ is the last BD to be decoded in the decoding order $\mathbf{Q}_n$, the expression of uplink data rate from $\mathrm{BD}_{k'}$ to BS_n is noted by

$$R_{n,k'}^{(\mathbf{Q}_n)} = \log_2\left(1 + \frac{\eta_{k'} P_{\mathrm{BD}_{k'}}\left|h_{n,k'}\right|^2}{I_{\mathrm{Inter}}(n) + \delta_n}\right). \tag{9}$$

The achievable sum data rate at BS_n is rewritten as

$$R_{\mathrm{BS},n} = \log_2\left(1 + \frac{\sum_{i=1}^{K} x_{n,i}\eta_i P_{\mathrm{BD}_i}\left|h_{n,i}\right|^2}{I_{\mathrm{Inter}}(n) + \delta_n}\right). \tag{10}$$

B. BENEFITS OF HYBRID SIC

The outage probability of the considered BackCom NOMA system is highly dependent on the decoding order, and hence, the corresponding optimization is crucial. The application of hybrid SIC enables dynamic adjustments to the decoding sequence, thereby preserving the fairness of system performance as evidenced by the sum rate of uplink data.

Proposition 1: Once the association strategy is determined, the decoding order of BDs which leads to the variant of the data rates of BDs cannot effect the sum-uplink data rate.

Proof: See Appendix A. ■

The decoding order of SIC can effect the uplink QoS of BDs individually. In the proposed system, if BD_{k_1} and BD_{k_2} are associated with BS_n and the decoding order of BD_{k_1} is superior than BD_{k_2} noted by $.\mathbf{Q}_n|_{k_1}^{k_2}$, the achievable uplink data rates from the BDs to their associated BS is given by:

$$\begin{cases} R_{n,k_1}^{\left(\mathbf{Q}_n|_{k_1}^{k_2}\right)} = \log_2\left(1 + \dfrac{\eta_{k_1} P_{\mathrm{BD}_{k_1}}\left|h_{n,k_1}\right|^2}{I_{\mathrm{Intra},n}^{\left(\mathbf{Q}_n|_{k_1}^{k_2}\right)}(k_1) + I_{\mathrm{Inter}}(n) \ + \delta_n}\right), & \text{(11a)} \\ R_{n,k_2}^{\left(\mathbf{Q}_n|_{k_1}^{k_2}\right)} = \log_2\left(1 + \dfrac{\eta_{k_2} P_{\mathrm{BD}_{k_2}}\left|h_{n,k_2}\right|^2}{I_{\mathrm{Intra},n}^{\left(\mathbf{Q}_n|_{k_1}^{k_2}\right)}(k_2) + I_{\mathrm{Inter}}(n) \ + \delta_n}\right). & \text{(11b)} \end{cases}$$

If the decoding order of BD_{k_1} and BD_{k_2} swapped which is noted by $.\mathbf{Q}_n|_{k_2}^{k_1}$, the achievable uplink data rates are formulated by:

$$\begin{cases} R_{n,k_1}^{\left(\mathbf{Q}_n|_{k_2}^{k_1}\right)} = \log_2\left(1 + \dfrac{\eta_{k_1} P_{\mathrm{BD}_{k_1}}\left|h_{n,k_1}\right|^2}{I_{\mathrm{Intra},n}^{\left(\mathbf{Q}_n|_{k_2}^{k_1}\right)}(k_1) + I_{\mathrm{Inter}}(n) \ + \delta_n}\right), & \text{(12a)} \\ R_{n,k_2}^{\left(\mathbf{Q}_n|_{k_2}^{k_1}\right)} = \log_2\left(1 + \dfrac{\eta_{k_2} P_{\mathrm{BD}_{k_2}}\left|h_{n,k_2}\right|^2}{I_{\mathrm{Intra},n}^{\left(\mathbf{Q}_n|_{k_2}^{k_1}\right)}(k_2) + I_{\mathrm{Inter}}(n) \ + \delta_n}\right). & \text{(12b)} \end{cases}$$

Namely, with the different decoding orders, the achievable uplink data rates for each BDs varies. Therefore, this part focuses on the fulfillment of $R_{n,k}$, leading to mitigation of the outage probability.

III. PROBLEM FORMULATION

This work aims to maximize the sum uplink data rate subject to the QoS constraints of UEs, where BD association, reflection coefficient and decoding order are studied. The optimization problem is formulated as follows

$$\begin{aligned} \max_{\mathbf{X},\boldsymbol{\eta},\mathcal{Q}} \quad & \sum_{n=1}^{N} R_{\mathrm{BS},n} && \text{(13a)} \\ \text{s.t.} \quad & R_{k,n}^{(\mathbf{Q}_n)} \geq R_{\mathrm{UL}}(k)\ , \forall n, && \text{(13b)} \\ & R_{n,0} \geq R_{\mathrm{DL}}, \forall n, && \text{(13c)} \\ & \sum_{i=1}^{N} x_{i,k} = 1, \forall k, && \text{(13d)} \\ & 0 \leq \eta_k \leq 1, \forall k, && \text{(13e)} \\ & x_{n,k} \in \{0, 1\}, \forall n, \forall k, && \text{(13f)} \end{aligned}$$

where $\mathbf{X} = \{x_{n,k}\}$ denotes the association coefficient set. $\boldsymbol{\eta} = [\eta_1, \ldots, \eta_K]^T$ denotes the collection of reflection coefficient. $R_{\mathrm{UL}}(k)$ denotes target uplink data rate from BD_k to BS_n and R_{DL} is the target downlink data rate for UE_n. (13b) means that the uplink data rate from BD_k to BS_n should be greater than or equal to the target data rate $R_{\mathrm{UL}}(k)$ of BD_k. (13c) indicates that the QoS of the downlink UEs should be guaranteed. Constraint (13d) implies that each BD can be

only associated with one BS. Due to the three optimization variables are coupled and the association index $\mathbf{X}$ is the integer variable and cannot be solved by CVX solvers, (13) is divided into two subproblems, including BD association problem and the reflection coefficient optimization problem.

A. BD ASSOCIATION PROBLEM

In BD association problem, (13c) can be ignored in the subproblem of association scheme. Due to all BDs receive the signals from all BSs, after the signals reflected by BDs which perform as the interference in all UEs, regardless the association scheme in this cell-free system. In the expression of (6), the association coefficients matrix $\mathbf{X}$ does not exists, which means that the downlink data rates has no relationships with the association scheme.

For the subproblem of optimizing BD association scheme, the variable $\boldsymbol{\eta}$ is considered to be known and the optimization problem is formulated as

$$\begin{aligned} \max_{\mathbf{X}} \quad & \sum_{n=1}^{N} R_{\mathrm{BS},n} \\ \text{s.t.} \quad & \text{(13d), (13f).} \end{aligned} \tag{14a}$$

In this work, the decoding order of BDs in the uplink is delegated to the power allocation problem, thereby obviating the need to consider the impact of hybrid SIC on BDs in the association context within (14). Consequently,the decoding order and constraint (13b) are excluded from consideration in this context.

B. RESOURCE ALLOCATION AND DECODING ORDER DESIGN

In order to decouple the subproblem which optimize the reflection indices and the decoding order, the optimization problem is formulated as:

$$\begin{aligned} \max_{\boldsymbol{\eta},\mathcal{Q}} \quad & \sum_{n=1}^{N} R_{\mathrm{BS},n} \\ \text{s.t.} \quad & \text{(13b), (13c), (13e).} \end{aligned} \tag{15a}$$

In (15), the reflection indices $\boldsymbol{\eta}$ and the decoding order $\mathcal{Q}$ are optimized iteratively until convergence. The term, $\boldsymbol{\eta}$, determines the decoding order $\mathcal{Q}$ and the decoding order $\mathcal{Q}$ has the impact on $\boldsymbol{\eta}$.

IV. ALGORITHM DESIGN

This section illustrates the approach adopted for maximizing the sum uplink data rate in the network under study. The problem presented is decomposed into two subproblems: the BD association problem and the resource allocation problem. To address the BD association issue, the method of matching theory is applied, providing a structured approach to efficiently pair BDs with appropriate network resources. For the resource allocation challenge, the quadratic transform technique is utilized. In addition to these methods, hybrid SIC is employed to optimize the decoding order. This strategy is implemented with the objective of reducing outage probability, while concurrently maintaining the performance of the sum uplink data rate. The combination of these techniques ensures an effective and efficient allocation of network resources, enhancing overall system performance.

A. MATCHING THEORY BASED BD ASSOCIATION

In this section, the application of matching theory, known for its low computational complexity, is explored to facilitate the interaction between BS and BDs. The discussion pivots on the unique sum uplink data rate maximization problems inherent to BackCom NOMA and BackCom OMA. Given its versatility, matching theory can be strategically applied to these two distinct optimization problems, thereby providing valuable insights for subsequent analyses and propositions.

The matching model under consideration between the BS and BDs falls within the purview of two-dimensional (2D) matching. Two disjoint sets, $\mathcal{N} = \{\mathrm{BS}_1, \ldots, \mathrm{BS}_N\}$ and $\mathcal{K} = \{\mathrm{BD}_1, \ldots, \mathrm{BD}_K\}$, $\mathcal{N} \cap \mathcal{K} = \varnothing$, are involved in this process. A matching operation is conducted wherein each element $n \in \mathcal{N}$ is associated with an element $k \in \mathcal{K}$. The nature of this association is consistent with a one-to-many matching model [28], shedding light on the dynamics of the matching process under discussion.

Definition 1: The one-to-many matching can be represented via a β-mapping function, which takes as its domain the combined set $\mathcal{N} \cup \mathcal{K}$ and maps it to the range comprising all elements within $\mathcal{N} \cup \mathcal{K}$. This function is defined such that:

1) $\beta(k) \in \mathcal{N}, \forall k \in \mathcal{K}, \beta(n) \in \mathcal{K}, \forall n \in \mathcal{N}$.
2) $|\beta(k)| = 1, \forall k \in \mathcal{K}, \sum_{n=1}^{N} |\beta(n)| = K, \forall n$.
3) $n = \beta(k) \Leftrightarrow k \in \beta(n)$.

The definition of the one-to-many matching function is proposed, where $|\beta(n)|$ denotes the number of the associated BDs for BS_n and the mapping β has the different meanings when the parameters varies. Condition 1) indicates that each BD associates with one of the BSs and each BS associates with the subset of the BDs. Condition 2) describes that each BD associates with one BS and all BDs are activated by their associated BDs. Condition 3) states that BD_k and BS_n are associated with each other.

In this scenario, considering the each BD is unselfish.[2] The notation, $\succ$, is introduced in this context to denote preference within matching theory. The expression $(k', \beta') \succ_n (k, \beta)$ conveys that for a given k, n exhibits a stronger preference to be matched with k', where β' and β denote the corresponding mapping from the BS to the BD. This paper is primarily focused on exploring the performance of sum uplink data rate, thus rendering sum uplink data rate as the determinant

2. This indicates that when a BD is switched to a new associated BS, the data rate of current BDs and UE will decrease. If this manner can increase the sum uplink data rate of the proposed BackCom NOMA system, all the BDs in the proposed cell will reduce their reflection coefficients in order to satisfy the downlink QoS constraint and the uplink QoS constraints.

of preference among various matching pairs. The preference relation is given by

$$\left(k', \beta'\right) \succ_n (k, \beta) \Leftrightarrow \mathcal{R}\left(\beta'\right) > \mathcal{R}(\beta), \tag{16}$$

where $\mathcal{R}(\beta)$ denotes the sum uplink data rate computation with the respect of the association scheme β. Similarly, the preference relation of the BD is expressed by

$$\left(n', \beta'\right) \succ_k (n, \beta) \Leftrightarrow \mathcal{R}\left(\beta'\right) > \mathcal{R}(\beta). \tag{17}$$

In the system under discussion, matching theory is pivotal to the process of associating BDs with BSs. This approach is different from the traditional two-sided exchange matching models referenced in [29] by implementing a switching operation as a fundamental mechanism. For instance, should BD_k initially be linked with BS_n, the application of matching theory would result in its re-association with a different BS, denoted as $\mathrm{BS}_{n'}$. Such transitions are designated by the notation $\beta_{(k_1,n_1)}^{(k_1,n_2)}$, representing the switch of BD_{k_1} from its current link with BS_{n_1} to a new link with BS_{n_2}, thus effectuating a singular switching operation. In the context of the multi-cell system under discussion, it is imperative to consider the dual nature of interference, encompassing both inter-cell and intra-cell types. Consequently, in scenarios where any BD undergoes re-association with a different BS, this action invariably influences the data rates of all users and BDs within the network. This interconnected impact underscores the complexity of the system, where individual changes can have wide-ranging effects on the overall network performance.

Definition 2: The mapping for switching operation matching is expressed by: $\beta_{(k_1,n_1)}^{(k_1,n_2)} = \{\beta \setminus (k_1, n_1)\} \cup (k_1, n_2)$, where $k_1 \in \beta(n_1)$ and $k_1 \in \beta_{(k_1,n_1)}^{(k_1,n_2)}(n_2)$.

The current mapping is given by $n_1 = \beta(k_1)$, when the switching operation is performed, the operation process can be expressed by $n_2 = \beta_{(k_1,n_1)}^{(k_1,n_2)}(k_1)$. During each iteration, the switching operation will not weaken sum uplink data rate performance. After traversing all the switching operations, the matching problem will eventually converge to the stable matching.

Definition 3: The matching β is the two-sided exchange stable if there is no swap blocking pair that satisfies the following conditions:

1) $\forall j \in \{k_1, n_1, n'\}$, $n' \in \beta(k_1)$, $n' \neq n_1$, $\mathcal{R}_j(\beta_{(k_1,n_1)}^{(k_1,n')}) \geq \mathcal{R}_i(\beta_{(k_1,n_1)}^{(k_1,n_2)})$,
2) $\exists j \in \{k_1, n_1, n'\}$, $n' \in \beta(k_1)$, $n' \neq n_1$, to ensure $\mathcal{R}_j(\beta_{(k_1,n_1)}^{(k_1,n')}) > \mathcal{R}_i(\beta_{(k_1,n_1)}^{(k_1,n_2)})$.

1) THE APPLICATION OF MATCHING THEORY

Within the established system model, the matching theory is utilized to accomplish the matching of BSs with BDs. The model stipulates that a single BS matches multiple BDs, with each BD being matched to a singular BS. The approach involves selecting a starting point that satisfies the one-to-many matching rule, and then iteratively performing a switch operation across all BDs until convergence is stable matching. The pseudo-code of this method is elaborated upon in **Algorithm** 1.

Algorithm 1: BDs Association Algorithm

Input : P_0, $\boldsymbol{\eta}$, $h_{n,k}$, $g_{n,k}$, $h_{\mathrm{SI},n}$, s_n, σ, α and the iteration recorder $i = 0$
Output: $\boldsymbol{X} \in \mathbb{R}^{N \times K}$

```
Randomly match BDs and BSs.
Initialize X, if BS_n is associated with BD_k, then x_{n,k} = 1, otherwise x_{n,k} = 0.
Record the current association scheme by β^(i).
while β^Before ≠ β^After do
    β^Before ← β^(i)
    while Search and select the random BD which is not performed before in this 'while' loop, do
        for n = 1:N and n ≠ β^(i)(k) do
            Switch BD_k to cluster n.
            if R(β^(i)) > R(β^(i−1)) then
                i ← i + 1
                Record β^(i).
                x_{n,k} ← 1 and x_{β^(i−1)(k),k} ← 0.
            end
        end
    end
    β^After ← β^(i)
end
```

At the inception of the algorithm, an association scheme is selected. Starting with BD_k, an exploration is conducted to ascertain whether associating BD_k with an unassociated BS would yield an improvement in system performance. If an enhancement is indeed observed, an association is established between BD_k and the given BS. Conversely, if there is no perceptible improvement in performance, the original association scheme is retained. The aforementioned steps are reiterated until the state of the association scheme is not changed. This process ensures an efficient association scheme is maintained, fostering improved system performance.

2) STARTING POINT SELECTION

In the context of matching theory, two schemes are presently available for the selection of the initial matching. One involves a random matching scheme, while the other utilizes a scheme where a BD chooses the BS closest in proximity. While the random matching scheme necessitates multiple iterations and delivers less-than-optimal performance, the minimum distance association scheme requires fewer iterations and exhibits better performance. The improved performance can be attributed to the initial choice being closer to the optimal matching scheme compared to that of the random matching scheme.

3) COMPLEXITY ANALYSIS

Utilizing matching theory to resolve the association between BSs and BDs demonstrates significantly lower complexity compared to exhaustive search methods. In the established system model presented herein, the complexity of exhaustive search stands at $\mathcal{O}(N^K)$. (14) serves as the optimization problem for addressing the association, wherein the variable of optimization, namely the association index $\mathbf{X}$, possesses a dimension of N^K. Concurrently, within the context of matching theory, $\mathbf{X}$ is subject to the constraints delineated in (13d) and (13f). Consequently, the complexity associated with **Algorithm** 1 is characterized as $\mathcal{O}(NK)$. Assuming the attainment of an optimal solution through $\mathcal{S}_{\text{mt}}$ iterations, where $1 \leq \mathcal{S}_{\text{mt}} \leq NK$, the algorithmic complexity of employing matching theory to solve (14) is thus expressed as $\mathcal{O}(\mathcal{S}_{\text{mt}}NK)$.

4) CONVERGENCE ANALYSIS

This section elucidates that the system's performance experiences continuous improvement through the application of matching theory. The alignment between BSs and BDs, fundamental to the architecture, is effectuated via a switch operation within the context of matching theory. Should there be a manifestation of superior system performance, particularly an enhancement in sum uplink data rate, the execution of the switch operation will be initiated. The procedure for executing the swap operation is described as follows

$$\beta^{(1)} \rightarrow \beta^{(2)} \rightarrow \beta^{(3)} \rightarrow \cdots \rightarrow \beta^{\text{final}}, \tag{18}$$

where $\beta^{(i)}$ denotes the i-th switch operation and β^{final} denotes the final convergence state. Consequently, with each iteration of the swap operation, an incremental advancement in performance is achieved. This continuous elevation in system efficiency can be expressed as

$$\mathcal{R}\left(\beta^{(1)}\right) < \mathcal{R}\left(\beta^{(2)}\right) < \mathcal{R}\left(\beta^{(3)}\right) < \cdots < \mathcal{R}\left(\beta^{\text{final}}\right). \tag{19}$$

5) STABILITY ANALYSIS

This section elucidates that by applying matching theory, specifically through the execution of switch operations, an optimum value can be achieved for a fixed set of reflection indices. In addressing the association scheme issue, the convergence analysis part of this study illustrates that the system's performance will experience continuous enhancement via swap operations. Given the mention of the maximum iteration count $\mathcal{S}_{\text{mt}}$, with the number of iterations equal to NK, it can be concluded that employing matching theory will definitively yield the optimal value for the method under consideration. Assuming that β^{final} is not stable would lead to the invalidation of **Definition** 3, implying the existence of at least one association strategy capable of enhancing system performance. Consequently, it is inferred that β^{final} is indeed stable.

B. QUADRATIC TRANSFORM BASED RESOURCE ALLOCATION AND DECODING ORDER DESIGN

In (15), the resource allocation problem is decoupled by the two optimization problem by adjusting the reflection coefficients and the decoding order for BDs. By adjusting the reflection coefficients and the decoding order for BDs iteratively, the optimal reflection coefficients and the decoding order will be found.

1) QUADRATIC TRANSFORM BASED RESOURCE ALLOCATION

Assume $\mathbf{a}_n = [x_{n,1}P_{\text{BD}_1}|h_{n,1}|^2, \ldots, x_{n,K}P_{\text{BD}_K}|h_{n,K}|^2]^T$, $\mathbf{b}_n = [(1-x_{n,1})P_{\text{BD}_1}|h_{n,1}|^2, \ldots, (1-x_{n,K})P_{\text{BD}_K}|h_{n,K}|^2]^T$, $\mathbf{c}_n = [P_{\text{BD}_1}|g_{n,1}|^2, \ldots, P_{\text{BD}_K}|g_{n,K}|^2]^T$, $\mathbf{d}_n(k) = [\mathbf{0}_{1\times k}, x_{n,k+1}P_{\text{BD}_{k+1}}|h_{n,k+1}|^2, \ldots, x_{n,K}P_{\text{BD}_K}|h_{n,K}|^2]^T$, and $\mathbf{f}_n(k) = [\mathbf{0}_{1\times(k-1)}, x_{n,k}P_{\text{BD}_k}|h_{n,k}|^2, \mathbf{0}_{1\times(K-k)}]^T$, the energy allocation optimization problem shown in (15) is recast as:

$$\max_{\boldsymbol{\eta}} \quad \sum_{n=1}^{N} \log_2\left(1 + \frac{\mathbf{a}_n^T\boldsymbol{\eta}}{\mathbf{b}_n^T\boldsymbol{\eta} + \delta_n}\right) \tag{20a}$$

$$\text{s.t.} \quad \gamma_{n,k}\left[\mathbf{d}_n^T(k)\ \boldsymbol{\eta} + \mathbf{b}_n^T\boldsymbol{\eta} + \delta_n\right] - \mathbf{f}_n^T(k)\ \boldsymbol{\eta} \leq 0, \quad \forall n, \tag{20b}$$

$$\gamma_n\left(\mathbf{c}_n^T\boldsymbol{\eta} + \sigma^2\right) - P_0\left|h_{n,0}\right|^2 \leq 0,\ \forall n, \tag{20c}$$

$$(13e),$$

where γ_k and γ_n denotes the target signal to interference-noise ratio (SINR) at BD_k and BS_n. The function defined in (20a) is characterized as non-convex, comprising a summation of logarithmic functions that incorporate fractional terms. Additionally, the elements within these fractions, both in the numerators and denominators, exhibit affine properties, and this characteristic extends to the constraints of the function as well. The knowledge of quadratic transform [30], [31] is applied to solve (20). (20) is recast as:

$$\max_{\boldsymbol{\eta}} \quad \sum_{n=1}^{N} \log_2\left[1 + 2q_n\sqrt{\mathbf{a}_n^T\boldsymbol{\eta}} - q_n^2\left(\mathbf{b}_n^T\boldsymbol{\eta} + \delta_n\right)\right]$$

$$\text{s.t.} \quad (13e), (20b), (20c), \tag{21a}$$

where q_n denotes the auxiliary variable and it is updated in each iteration by:

$$q_n^\star = \frac{\sqrt{\mathbf{a}_n^T\boldsymbol{\eta}}}{\mathbf{b}_n^T\boldsymbol{\eta} + \delta_n}. \tag{22}$$

Proposition 2: Eq. (21a) is a concave function.

Proof: See Appendix B. ■

Due to (21a) is a concave function. Therefore, (21) can be solve by some toolbox in MATLAB, i.e., CVX. To get the optimal reflection coefficient $\boldsymbol{\eta}^\star$, the value of $\boldsymbol{\eta}$ and q_n need to be updated iteratively. Firstly, the random reflection coefficient $\boldsymbol{\eta}_{(0)}$ which is in the feasible set needs to be found. Secondly, update q_n with (22). Then, update the variable $\boldsymbol{\eta}$ with the obtained q_n by solving (21) in sequence until convergence. The optimal reflection coefficient $\boldsymbol{\eta}^\star$ will be

Algorithm 2: Quadratic Transform

Input : $\mathbf{a}_n$, $\mathbf{b}_n$, $\mathbf{c}_n$, α, P_0, δ_n, q_n, stopping criterion ζ and the rounds for iteration $k = 1$

. **Output**: $\boldsymbol{\eta}$

Initialize $\boldsymbol{\eta}$ and the objective value $p_{(0)} = 0$.

while $p > \zeta$ **do**

  Optimize (21) and obtain $\boldsymbol{\eta}$.

  Update q_n by (22).

  Compute the optimal objective value $p_{(k)}$.

  $p = \left|p_{(k)} - p_{(k-1)}\right|$.

  $k \leftarrow k + 1$

end

obtained. The pseudocode for hunting optimal $\boldsymbol{\eta}^{\star}$ is shown in **Algorithm** 2.

The quadratic transform which is listed in **Algorithm** 2 provides an effective method for solving the non-convex optimization problem in (21). The algorithm iteratively updates the auxiliary variable q_n and the reflection coefficients $\boldsymbol{\eta}$ to find the optimal solution. By initializing $\boldsymbol{\eta}$ and setting a stopping criterion ζ, the algorithm converges when the difference between successive optimal objective values is less than the specified threshold ζ. This approach ensures that a near-optimal solution can be found in a reasonable amount of time, making it suitable for practical applications in BackCom NOMA systems.

2) SIC DECODING ORDER DESIGN

In the following, a threshold $I_{\max,n}(k)$ associated with interference power from coded BDs related to BS_n is first introduced when decoding the signal from BD_k, when the interference is equal to $I_{\max,n}(k)$, the achievable data rate for BD_k is equal to its target rate, where can be expressed by

$$\frac{\eta_k P_{\mathrm{BD}_k}\left|h_{n,k}\right|^2}{I_{\max,n}(k) + I_{\mathrm{Inter}}(n) + \delta_n} = \gamma_k. \tag{23}$$

Therefore, the expression of $I_{\max,n}(k)$ is formulated by

$$I_{\max,n}(k) = \frac{\eta_k P_{\mathrm{BD}_k}\left|h_{n,k}\right|^2}{\gamma_k} - I_{\mathrm{Inter}}(n) - \delta_n. \tag{24}$$

When BD_k is decoded last noted by $\mathbf{Q}'_n$, the uplink SINR from BD_k to BS_n reaches its maximum. Under these circumstances, the SINR is equivalent to the SINR of BD_k which is the only BD in the cluster n, which can be represented as

$$R_{n,k}^{(\mathbf{Q}'_n)} = \frac{\eta_k P_{\mathrm{BD}_k}\left|h_{n,k}\right|^2}{I_{\mathrm{Inter}}(n) + \delta_n}. \tag{25}$$

Therefore, when $R_{n,k}^{(\mathbf{Q}'_n)} < R_{\mathrm{UL}}(k)$, the maximum interference power for BD_k to its associated BS_n is set to 0, i.e., $I_{\max,n}(k) = 0$. Given the aforementioned two possibilities, the expression for $I_{\max,n}(k)$ can be succinctly represented as

$$I_{\max,n}(k) = \max\left\{0, \frac{\eta_k P_{\mathrm{BD}_k}\left|h_{n,k}\right|^2}{\gamma_k} - I_{\mathrm{Inter}}(n) - \delta_n\right\}. \tag{26}$$

Remark 1: In certain scenarios, even if the BD_k is the last order to be decoded, the data rate of BD_k is still falls below the target data rate, resulting in system interruption; hence, in the BackCom NOMA system, the outage performance is equivalent to that in the BackCom OMA system, i.e.,

$$\mathbb{P}\left(R_{n,k} < R_k\right) = \mathbb{P}\left(R_{n,k}^{(\mathbf{Q}'_n)} < R_k\right) = 1. \tag{27}$$

Proof: The target rate for BD_k is the last order to be decoded in cluster n is smaller than its target data rate means that the maximum achievable data rate of BD_k is smaller than its target data rate, i.e.,

$$R_{n,k}^{(\mathbf{Q}'_n)} < R_k. \tag{28}$$

In other words, ignoring the decoding order for BD_k, it is impossible to reach its target data rate. This indicates that the achievable uplink data rate for BD_k will definitely not equal or higher than its target data rate, resulting in the outage of the uplink transmission for BD_k. ■

During the implementation of hybrid SIC, five factors are taken into account according to the relationships between $P_{\mathrm{coded},n}(k)$ and $I_{\max,n}(k)$.

- Factor I: If $I_{\mathrm{Intra},n}^{(\mathbf{Q}_n)}(k) > I_{\max,n}(k)$ and $I_{\max,n}(k) = 0$, $R_{n,k}^{(\mathbf{Q}_n)} < R_k$, which means that the achievable data rate for BD_k will definitely not satisfy its target rate, resulting the outage of the link from BD_k to BS_n. Therefore, for the better QoS of the other BDs, this kind of BDs will be decoded first.
- Factor II: If $I_{\mathrm{Intra},n}^{(\mathbf{Q}_n)}(k) = I_{\max,n}(k)$ and $I_{\max,n}(k) = 0$, this means that $\max\{R_{n,k}^{(\mathbf{Q}_n)}|\forall\mathbf{Q}_n\} = R_{n,k}^{(\mathbf{Q}'_n)}$. These BDs should be decoded last. If more than one BDs satisfy this case, the maximum value of $\eta_k P_{\mathrm{BD}_k}|h_{n,k}|^2$ related to BD_k will be decoded first among this kind of BDs, to endeavour to reduce more intra-cell interference for other coded BDs.
- Factor III: If $I_{\mathrm{Intra},n}^{(\mathbf{Q}_n)}(k) > I_{\max,n}(k)$ and $I_{\max,n}(k) \neq 0$, the decoding order $\mathbf{Q}_n$ needs to be adjusted until $P_{\mathrm{coded},n}^{(\mathbf{Q}'_n)}(k) \leq I_{\max,n}(k)$.
- Factor IV: If $I_{\mathrm{Intra},n}^{(\mathbf{Q}_n)}(k) \leq I_{\max,n}(k)$ and $I_{\max,n}(k) - I_{\mathrm{Intra},n}^{(\mathbf{Q}_n)}(k) > \min\{I_{\max,n}(k) - I_{\mathrm{Intra},n}^{(\mathbf{Q}_n)}(k)|\forall\mathbf{Q}_n\}$, adjusting the decoding order of BD_k, until $I_{\max,n}(k) - I_{\mathrm{Intra},n}^{(\mathbf{Q}_n)}(k) = \min\{I_{\max,n}(k) - I_{\mathrm{Intra},n}^{(\mathbf{Q}_n)}(k)|\forall\mathbf{Q}_n\}$.
- Factor V: If $I_{\mathrm{Intra},n}^{(\mathbf{Q}_n)}(k_1) > I_{\max,n}(k_1)$, $I_{\mathrm{Intra},n}^{(\mathbf{Q}_n)}(k_2) > I_{\max,n}(k_2)$ and $I_{\max,n}(k_1) = I_{\max,n}(k_2) = 0$, the decoding order of BD_{k_1} and BD_{k_2} becomes inconsequential as neither the BDs can achieve the target SINR, thereby imparting no influence on the system performance.

From the five factors above, the conclusion for the expression of the outage probability can be given by

$$\mathbb{P}\left(R_{n,k}^{(\mathbf{Q}_n)} < R_k\right) = \begin{cases} 1,\ I_{\max,n}(k) < I_{\text{Inter}}(n) + \delta_n, & \text{(29a)} \\ \dfrac{I_{\text{Intra},n}^{(\mathbf{Q}_n)}(k)}{I_{\text{Inter}}(n) + \delta_n + I_{\text{Intra},n}^{(\mathbf{Q}_n)}(k)},\ I_{\text{Inter}}(n) & \\ \quad +\delta_n \le I_{\max,n}(k) \le I_{\text{Inter}}(n) & \\ \quad +\delta_n + I_{\text{Intra},n}^{(\mathbf{Q}_n)}(k), & \text{(29b)} \\ 0,\ I_{\max,n}(k) \ge & \\ \quad I_{\text{Inter}}(n) + \delta_n + I_{\text{Intra},n}^{(\mathbf{Q}_n)}(k). & \text{(29c)} \end{cases}$$

Proposition 3: In the implementation of hybrid SIC, the decoding order at the BS_n is determined by the magnitude of $I_{\max,n}(k)$, with signals from BD_k with larger $I_{\max,n}(k)$ being decoded earlier.

Proof: See Appendix C. ∎

Proposition 4: Hybrid SIC can mitigate the outage probabilities in the proposed system compared with conventional SIC.

Proof: See Appendix D. ∎

In the context of power allocation for this system, the inability to determine the decoding order for the uplink introduces a level of complexity. To address this, an iterative algorithm is employed to identify the optimal decoding order and reflection coefficients. The alternating optimization of these two parameters allows for the extraction of the optimal solution for both. Initially, a random decoding order for the BDs is chosen for each BS. If this decoding order renders (21) infeasible, a new set of decoding orders is generated. Conversely, if the decoding order enables feasibility for (21), then the optimal reflection coefficients are determined based on this decoding order through the proposed iterative algorithm (21) and (22). Subsequently, using the derived reflection coefficients, a new decoding order is selected. This approach enables a flexible and dynamic optimization strategy that effectively addresses the challenges posed by the uncertain decoding order in the uplink. As reflection coefficients $\boldsymbol{\eta}$ are already determined in this subproblem, and the target uplink data rate remains consistent for various BDs, decoding order is established based on the magnitude of $I_{\max,n}(k)$. For example, BS_n associates with BD_1, BD_2, BD_3, and $I_{\max,n}(1) > I_{\max,n}(2) > I_{\max,n}(3)$, therefore, the decoding order is BD_1, BD_2, BD_3, respectively. By repeating generating the new decoding order and solving the reflection coefficients iteratively, the optimum decoding order and the reflection coefficients will obtained.

Remarkably, this decoding methodology does not exert any influence on the overall uplink rate of the proposed system model. Thus, it effectively maintains system performance while enhancing outage probability, confirming the efficiency of hybrid SIC in energy allocation scenarios.

3) COMPLEXITY ANALYSIS

Equation (21) embodies three distinct constraints, delineated in (20b), (20c), and (13e). The variables optimized in this context are the reflection indices, symbolized as $\boldsymbol{\eta}$, incorporating K individual elements. As (20b) is limited to the discussion of BD_k and its corresponding matched BS_n, it houses K inequalities. Further, (20c) comprises N inequalities, and (13e) includes K inequalities. Thus, the computational complexity for resolving (21) stands at $\mathcal{O}(K^2 + NK + K)$. Within the framework of **Algorithm 2**, a specific stopping criterion, represented by ξ, is instituted. As such, the complexity associated with solving the resource allocation conundrum is $\mathcal{O}[-\log_2 \xi(K^2 + NK + K)]$. Considering the deployment of hybrid SIC, and recognizing the determined decoding sequence that alternates optimization with the resource allocation dilemma, the complexity for achieving the optimal decoding sequence and $\boldsymbol{\eta}^\star$ within the proposed algorithm is quantified as $\mathcal{O}[(\log_2 \xi)^2(K^2 + NK + K)]$. Considering optimizing the association indices, the reflection coefficients and the decoding order for BDs simultaneously, the complexity of iterative optimization between (14) and (15) is given by $\mathcal{O}[-\mathcal{S}_{\text{mt}}(\log_2 \xi)^3(NK^3 + N^2K^2 + NK^2)]$.

Algorithm 3: The Iterative Optimization for Reflection Coefficients and Decoding Order

Input : $\mathbf{a}_n$, $\mathbf{b}_n$, $\mathbf{c}_n$, α, P_0, δ_n, q_n and stopping criterion ζ.
Output: $\mathcal{Q}$

```
Initialize Q.
while p > ζ do
    Update η by Algorithm 2.
    Update Q based on the magnitude of I_{max,n}(i).
    Compute the optimal objective value p_(k).
    p = p_(k) − p_(k−1).
end
```

V. SIMULATION RESULTS

In this section, six figures are demonstrated to show the superiority of the mentioned algorithms. In this simulation, the number of the BSs is 4 and the location of the BSs are $(3, 3)$, $(3, -3)$, $(-3, 3)$, $(-3, -3)$. BDs are evenly scattered in the circle of a radius of 3 centered on the origin $(0, 0)$, UE_n is located on the extension line from the origin to BS_n, and the distance between UE_n and BS_n is 1. The large-scale pathloss model of [32] is applied and the pathloss coefficient α_{PL} is set to -3, the pathloss is expressed by $\beta = d^{\alpha_{\text{PL}}}$, where d is the distance between the end points. The small-scale multipath fading is also considered. The thermal noise is set to -94 dBm. The transmit power is 20 dBm. The self-interference coefficient is 10^{-4}. The target uplink data rate is set to randomly distributed from 0.1 to 0.9 bit per channel use (BPCU). The target downlink data rate is the random data rate between 0 and 1 BPCU. The Monte Carlo simulation is performed and the following results are obtained.

Fig. 2 illustrates how the iterative optimization performs in the proposed BackCom NOMA system to get the

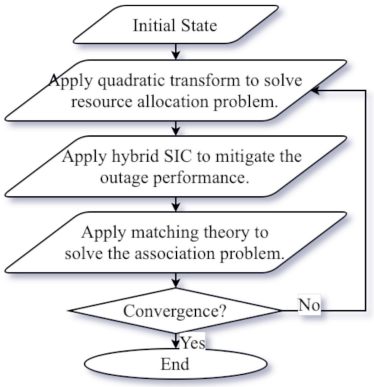

FIGURE 2. Flow chart on the iterative optimization.

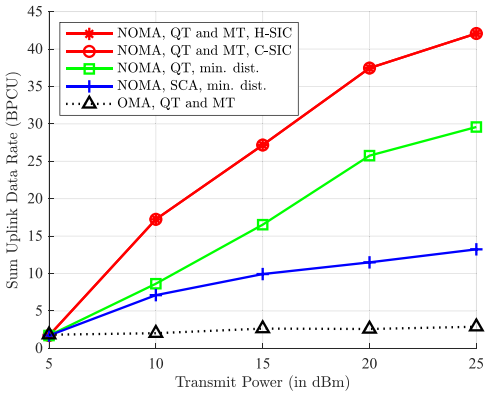

(a) The sum uplink data rate verses the transmit power (P_0).

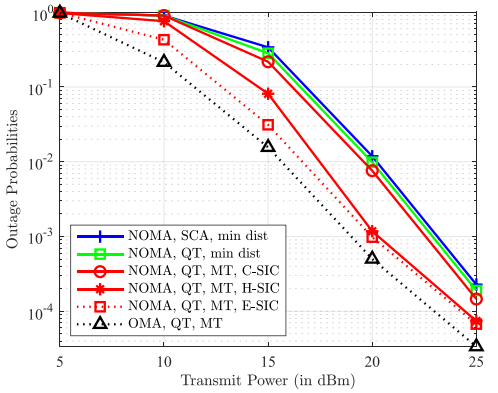

(b) Outage performance analysis when the transmit power (P_0) varies.

FIGURE 3. Performance analysis when the transmit power (P_0) varies.

maximal sum uplink data rate. The original association scheme is that BDs associate with their nearest BDs. Then, quadratic transform is applied to solve the resource allocation problem and hybrid SIC is implemented to reduce outage performance. After that, matching theory is applied to handle the BDs association problem. When the sum uplink data rate convergence, the iterative optimization between (14) and (15) terminates. In the original optimization problem (13), two distinct variables are involved: the matching coefficients and reflection coefficients. As these two variables operate independently, alternative optimization can be employed. This approach derives a global optimal solution through the alternative optimization of matching theory and quadratic transform.

In a setup with 12 BDs, Fig. 3 and Fig. 3(a) analyze the impact of BS transmission power on system performance and uplink rate. Fig. 3(b) confirms that decoding orders do not significantly affect the system's sum uplink rate, and an enhancement is observed with increased BS power. The proposed optimization algorithm outperforms the minimum distance association and successive convex approximation (SCA) benchmarks. Notably, the BackCom NOMA system surpasses the BackCom OMA in performance. Conversely, Fig. 3(b) shows reduced outage probability with higher transmission power. Among algorithms, conventional SIC displays the highest outage probability, especially against the proposed decoding order. As BS power rises, the proposed scheme's performance starts resembling exhaustive search outcomes, albeit the latter's higher complexity.

For a setup with 12 BDs, Fig. 4 and Fig. 4(a) analyze the effect of downlink target data rates on system and uplink rate performance. Fig. 4(a) confirms that varying decoding orders don't significantly alter the system's sum uplink rate. However, a rise in the downlink target data rate causes a decrease in the sum uplink rate, due to the need to minimize reflection coefficient, which reduces interference to the downlink user. Compared to the benchmarks like the minimum distance association and SCA, the proposed optimization algorithm shows enhanced efficacy. The BackCom NOMA system also displays a notable performance advantage over the BackCom OMA. Meanwhile, Fig. 4(b) indicates that a higher downlink target data rate boosts the system's outage probability due to reduced reflection coefficients. Conventional SIC showcases the highest outage probability, especially when compared to the proposed decoding order.

At a transmission power of 25 dBm for BSs, Fig. 5, Fig. 5(a) and Fig. 5(c) explore the effects of varying BD numbers on system and uplink rate performance. The two scenarios of the different BS deployment are discussed, i.e., the proposed 4-BS deployment and the 3-BS deployment whose BSs are located in $(0, 3)$, $(-\frac{3}{2}\sqrt{3}, -\frac{3}{2})$ and $(\frac{3}{2}\sqrt{3}, -\frac{3}{2})$, respectively. Fig. 5(a) and Fig. 5(c) verify that different decoding orders negligibly influence the system's sum uplink rate, yet a rise in the downlink target data rate boosts the uplink rate. The proposed optimization algorithm outperforms benchmarks like the minimum distance association and random reflection indices, with the BackCom NOMA system outshining the BackCom OMA. Meanwhile, Fig. 5(b) and Fig. 5(d) highlight that increasing BDs amplifies outage probability, due to factors like downlink user data rate constraints and heightened intra-cell interference. Conventional SIC, among strategies, registers the highest

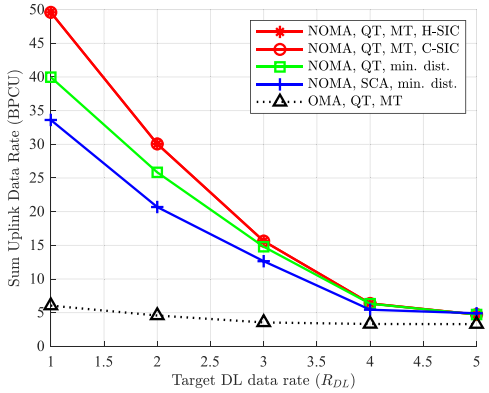

(a) The sum uplink data rate verses the downlink data rate (R_{DL}).

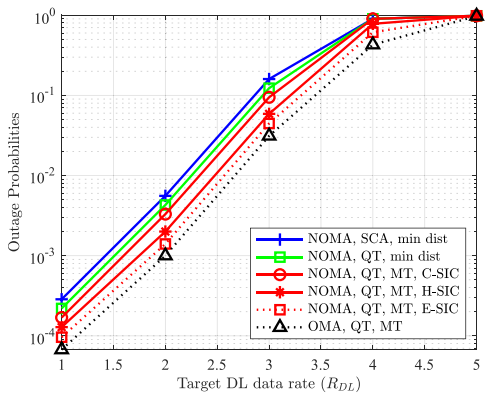

(b) Outage performance analysis when the downlink data rate (R_{DL}) varies.

FIGURE 4. Performance analysis when the downlink data rate (R_{DL}) varies.

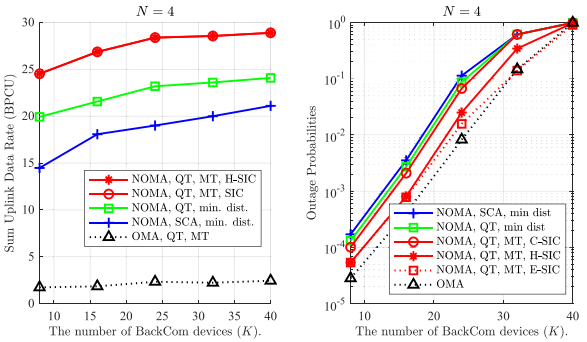

(a) The sum uplink data rate verses the number of BDs (K) when $N = 4$.

(b) Outage performance analysis when the number of BDs (K) varies and $N = 4$.

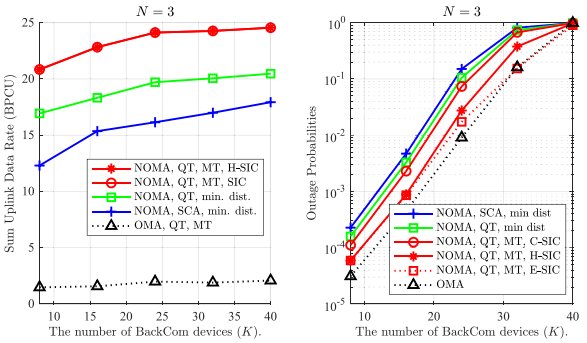

(c) The sum uplink data rate verses the number of BDs (K) when $N = 3$.

(d) Outage performance analysis when the number of BDs (K) varies and $N = 3$.

FIGURE 5. Performance analysis when the number of BDs (K) varies.

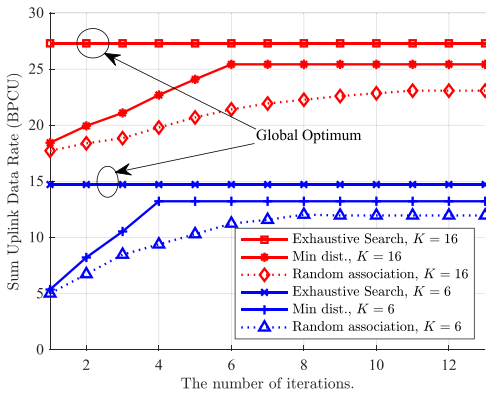

FIGURE 6. The convergence analysis with different original association scheme determination.

outage probability. Notably, the proposed algorithm effectively mitigates outage probability, especially at lower BD counts, closely matching exhaustive search outcomes.

In the considered framework, the transmission power of the BS is set to 25 dBm. Fig. 6 presents an analysis of the impact of different initial points of iteration on the sum uplink data rate and the number of iterations required. For this analysis, the results obtained from exhaustive research are used as the upper bound. It is observed that employing the minimum distance association scheme as the starting point of iteration leads to improved convergence and yields a higher sum uplink data rate. Additionally, as the number of BD increases, the system performance improves, with the minimum distance association scheme showing a corresponding enhancement. Interestingly, starting the iteration with the minimum distance association scheme achieves 93% of the performance level, requiring only 3.4 minutes of computation time, in contrast to the exhaustive search method, which necessitates 5.74 hours when $K = 16$ and $N = 3$. It is important to note that the iterative processes of exhaustive search and matching theory are not at the same level of computational complexity, hence are not directly comparable. Hence, the matching theory proves to be significantly more efficient than exhaustive search for this system configuration.

VI. CONCLUSION

In this work, a system model was established that is based on NOMA, integrating multiple BSs, BDs, and UEs. Through the synergistic application of matching theory and the quadratic transform iterative algorithm, the maximum sum uplink rate was achieved. In particular, the utilization of hybrid SIC in the uplink part effectively reduced outage

probabilities, thereby making the optimization problem more feasible. Simulation results indicated that the BackCom NOMA system outperforms the BackCom OMA in terms of performance. The use of hybrid SIC further contributed to lowering outage probabilities. This work indicates that the combination of matching theory with the quadratic transform iterative algorithm led to the system reaching its optimal performance. In forthcoming studies, we intend to investigate the optimization of beamforming and reflection coefficients within BackCom NOMA systems operating in low latency scenarios or imperfect channel state information, striving to create a framework that not only mirrors real-life conditions more precisely but also augments the system functionality in time-sensitive applications.

APPENDIX A
PROOF OF PROPOSITION 1

The uplink data rate for BD_k is given in (7) and (9). The term in the logarithm function which is formulated by

$$\left(1+\frac{\eta_k P_{\mathrm{BD}_k}\left|h_{n,k}\right|^2}{I_{\mathrm{Intra},n}^{(\mathbf{Q}_n)}(k)+I_{\mathrm{Inter}}(n)+\delta_n}\right) = \frac{\sum_{i=k}^{K}\eta_i P_{\mathrm{BD}_i}\left|h_{n,i}\right|^2+I_{\mathrm{Inter}}(n)+\delta_n}{I_{\mathrm{Intra},n}^{(\mathbf{Q}_n)}(k)+I_{\mathrm{Inter}}(n)+\delta_n}. \tag{30}$$

The uplink data rate for BS_n is given in (10). Therefore, the sum uplink data rate for decoding order $\mathbf{Q}_n$ is given by

$$\begin{aligned} R_{\mathrm{BS},n}^{(\mathbf{Q}_n)} &= \sum_{k=1}^{K}\log_2\left(\frac{\sum_{i=k}^{K}\eta_i P_{\mathrm{BD}_i}\left|h_{n,i}\right|^2+I_{\mathrm{Inter}}(n)+\delta_n}{I_{\mathrm{Intra},n}^{(\mathbf{Q}_n)}(k)+I_{\mathrm{Inter}}(n)+\delta_n}\right) \\ &= \log_2\left(\frac{\sum_{i=1}^{K}\eta_i P_{\mathrm{BD}_i}\left|h_{n,i}\right|^2+I_{\mathrm{Inter}}(n)+\delta_n}{I_{\mathrm{Intra},n}^{(\mathbf{Q}_n)}(1)+I_{\mathrm{Inter}}(n)+\delta_n}\cdots \right. \\ &\qquad \left. \frac{\eta_K P_{\mathrm{BD}_K}\left|h_{n,K}\right|^2+I_{\mathrm{Inter}}(n)+\delta_n}{I_{\mathrm{Inter}}(n)+\delta_n}\right) \\ &= \log_2\left(1+\frac{\sum_{i=1}^{K}\eta_i P_{\mathrm{BD}_i}\left|h_{n,i}\right|^2}{I_{\mathrm{Inter}}(n)+\delta_n}\right). \end{aligned} \tag{31}$$

Eq. (31) does not include the decoding order $\mathbf{Q}_n$, therefore, the uplink sum data rate is not affected by the decoding order. Similarly, the sum uplink data rate with any other decoding order $\mathbf{Q}_{n'}$ is given by

$$R_{\mathrm{BS},n}^{(\mathbf{Q}_{n'})} = \log_2\left(1+\frac{\sum_{i=1}^{K}\eta_i P_{\mathrm{BD}_i}\left|h_{n,i}\right|^2}{I_{\mathrm{Inter}}(n)+\delta_n}\right). \tag{32}$$

The expression of the sum uplink data rate given in (31) is equivalent to (10) and (7). And the decoding order does not have the impact on the performance of the proposed system.

APPENDIX B
PROOF OF PROPOSITION 2

The objective function is given in (21a). Assume $f(\boldsymbol{\eta}) = \log_2\left[1+2q_n\sqrt{\mathbf{a}_n^T\boldsymbol{\eta}}-q_n^2(\mathbf{b}_n^T\boldsymbol{\eta}+\delta_n)\right]$. The derivation of $f(\boldsymbol{\eta})$ is given by

$$f'(\boldsymbol{\eta}) = \frac{1}{\ln 2}\frac{q_n\mathbf{a}_n\left(\mathbf{a}_n^T\boldsymbol{\eta}\right)^{-\frac{1}{2}}-q_n^2\mathbf{b}_n}{1+2q_n\sqrt{\mathbf{a}_n^T\boldsymbol{\eta}}-q_n^2\left(\mathbf{b}_n^T\boldsymbol{\eta}+\delta_n\right)}. \tag{33}$$

Assume $\mathbf{g}(\boldsymbol{\eta}) = q_n\mathbf{a}_n(\mathbf{a}_n^T\boldsymbol{\eta})^{-\frac{1}{2}}-q_n^2\mathbf{b}_n$, $h(\boldsymbol{\eta}) = 1+2q_n\sqrt{\mathbf{a}_n^T\boldsymbol{\eta}}-q_n^2(\mathbf{b}_n^T\boldsymbol{\eta}+\delta_n)$, and $h'(\boldsymbol{\eta})=\mathbf{g}(\boldsymbol{\eta})$. Therefore, the derivative of $\frac{\mathbf{g}(\boldsymbol{\eta})}{h(\boldsymbol{\eta})}$ is

$$d\left[\frac{\mathbf{g}(\boldsymbol{\eta})}{h(\boldsymbol{\eta})}\right] = \frac{-\frac{1}{2}q_n\mathbf{a}_n\mathbf{a}_n^T\left(\mathbf{a}_n^T\boldsymbol{\eta}\right)^{-\frac{3}{2}}-\mathbf{g}(\boldsymbol{\eta})\mathbf{g}^T(\boldsymbol{\eta})}{h^2(\boldsymbol{\eta})}. \tag{34}$$

Due to $\mathbf{a}_n \succeq \mathbf{0}$ and $\boldsymbol{\eta}\succeq\mathbf{0}$, $\mathbf{a}_n^T\boldsymbol{\eta}\geq 0$, therefore,

$$d\left[\frac{\mathbf{g}(\boldsymbol{\eta})}{h(\boldsymbol{\eta})}\right] \preceq \mathbf{0}. \tag{35}$$

$f''(\boldsymbol{\eta})\preceq\mathbf{0}$, hence, (21a) is concave.

APPENDIX C
PROOF OF PROPOSITION 3

Assume two BDs, BD_{k_1} and BD_{k_2}, are associated with BS_n, $I_{\max,n}(k)\neq 0$, $\forall k$, $I_{\max,n}(k_1) > I_{\max,n}(k_2)$. If the decoding order for BD_{k_1} is superior to BD_{k_2}, which is noted by $.\mathbf{Q}_n|_{k_1}^{k_2}$, the outage probability error floors are given by

$$\begin{cases} \mathbb{P}\left(R_{n,k_1}^{\left(\mathbf{Q}_n|_{k_1}^{k_2}\right)} < R_{k_1}\right) = \mathbb{P}\left(I_{\mathrm{Intra},n}^{\left(\mathbf{Q}_n|_{k_1}^{k_2}\right)}(k_1) > I_{\max,n}(k_1)\right), & \text{(36a)} \\ \mathbb{P}\left(R_{n,k_2}^{\left(\mathbf{Q}_n|_{k_1}^{k_2}\right)} < R_{k_2}\right) = \mathbb{P}\left(I_{\mathrm{Intra},n}^{\left(\mathbf{Q}_n|_{k_1}^{k_2}\right)}(k_2) > I_{\max,n}(k_2)\right). & \text{(36b)} \end{cases}$$

If the decoding order for BD_{k_1} and BD_{k_2} is swapped, which is noted by $.\mathbf{Q}_n|_{k_2}^{k_1}$, the outage probability error floors are given by

$$\begin{cases} \mathbb{P}\left(R_{n,k_1}^{\left(\mathbf{Q}_n|_{k_2}^{k_1}\right)} < R_{k_1}\right) = \mathbb{P}\left(I_{\mathrm{Intra},n}^{\left(\mathbf{Q}_n|_{k_2}^{k_1}\right)}(k_1) > I_{\max,n}(k_1)\right), & \text{(37a)} \\ \mathbb{P}\left(R_{n,k_2}^{\left(\mathbf{Q}_n|_{k_2}^{k_1}\right)} < R_{k_2}\right) = \mathbb{P}\left(I_{\mathrm{Intra},n}^{\left(\mathbf{Q}_n|_{k_2}^{k_1}\right)}(k_2) > I_{\max,n}(k_2)\right). & \text{(37b)} \end{cases}$$

Case I: $\mathbb{P}(R_{n,k_1}^{(\mathbf{Q}_n)}\leq R_{k_1})=0$ and $\mathbb{P}(R_{n,k_2}^{(\mathbf{Q}_n)}\leq R_{k_2})<1$. In this case,

$$\begin{cases} \mathbb{P}\left(R_{n,k_1}^{\left(\mathbf{Q}_n|_{k_1}^{k_2}\right)} < R_{k_1}\right) = 0, & \text{(38a)} \\ \mathbb{P}\left(R_{n,k_2}^{\left(\mathbf{Q}_n|_{k_1}^{k_2}\right)} < R_{k_2}\right) \leq 1, & \text{(38b)} \end{cases}$$

and

$$\begin{cases} \mathbb{P}\left(R_{n,k_1}^{\left(\mathbf{Q}_n|_{k_2}^{k_1}\right)} < R_{k_1}\right) = 0, & (39a) \\ \mathbb{P}\left(R_{n,k_2}^{\left(\mathbf{Q}_n|_{k_2}^{k_1}\right)} < R_{k_2}\right) \leq 1. & (39b) \end{cases}$$

Namely, $R_{n,k_2}^{(\mathbf{Q}_n|_{k_1}^{k_2})} \leq R_{n,k_2}^{(\mathbf{Q}_n|_{k_2}^{k_1})}$, which means that $\mathbb{P}(R_{n,k_1}^{(\mathbf{Q}_n|_{k_2}^{k_1})} < R_{k_1}) = \mathbb{P}(R_{n,k_1}^{(\mathbf{Q}_n|_{k_1}^{k_2})} < R_{k_1}) = 0$. And $I_{\text{Intra},n}^{(\mathbf{Q}_n|_{k_1}^{k_2})}(k_2) < I_{\text{Intra},n}^{(\mathbf{Q}_n|_{k_2}^{k_1})}(k_2)$, therefore, $\mathbb{P}(R_{n,k_2}^{(\mathbf{Q}_n|_{k_1}^{k_2})} < R_{k_2}) < \mathbb{P}(R_{n,k_2}^{(\mathbf{Q}_n|_{k_2}^{k_1})} < R_{k_2}) < 1$.

Case II: $\mathbb{P}(R_{n,k_1}^{(\mathbf{Q}_n)} \leq R_{k_1}) < 1$ and $\mathbb{P}(R_{n,k_2}^{(\mathbf{Q}_n)} \leq R_{k_2}) < 1$. In this case,

$$\begin{cases} \mathbb{P}\left(R_{n,k_1}^{\left(\mathbf{Q}_n|_{k_1}^{k_2}\right)} < R_{k_1}\right) \leq 1, & (40a) \\ \mathbb{P}\left(R_{n,k_2}^{\left(\mathbf{Q}_n|_{k_1}^{k_2}\right)} < R_{k_2}\right) \leq 1, & (40b) \end{cases}$$

and

$$\begin{cases} \mathbb{P}\left(R_{n,k_1}^{\left(\mathbf{Q}_n|_{k_2}^{k_1}\right)} < R_{k_1}\right) \leq 1, & (41a) \\ \mathbb{P}\left(R_{n,k_2}^{\left(\mathbf{Q}_n|_{k_2}^{k_1}\right)} < R_{k_2}\right) \leq 1. & (41b) \end{cases}$$

As $I_{\text{Intra},n}^{(\mathbf{Q}_n|_{k_1}^{k_2})}(k_1) > I_{\text{Intra},n}^{(\mathbf{Q}_n|_{k_2}^{k_1})}(k_1)$ and $I_{\text{Intra},n}^{(\mathbf{Q}_n|_{k_1}^{k_2})}(k_2) < I_{\text{Intra},n}^{(\mathbf{Q}_n|_{k_2}^{k_1})}(k_2)$, $\mathbb{P}(R_{n,k_1}^{(\mathbf{Q}_n|_{k_1}^{k_2})} < R_{k_1}) > \mathbb{P}(R_{n,k_1}^{(\mathbf{Q}_n|_{k_2}^{k_1})} < R_{k_1})$ and $\mathbb{P}(R_{n,k_2}^{(\mathbf{Q}_n|_{k_1}^{k_2})} < R_{k_2}) < \mathbb{P}(R_{n,k_2}^{(\mathbf{Q}_n|_{k_2}^{k_1})} < R_{k_2})$. While the outage performance presented does not change, to lower the complexity of the decoding order, the principle mentioned in Proposition 3 can still be applied while the outage performance will not change.

In all, the term $I_{\max,n}(k)$ gauges the tolerance to the interference generated by coded BDs when decoding the uplink signal from BD_k, hence the larger the $I_{\max,n}(k)$, the higher the priority of BD_k in the decoding sequence.

APPENDIX D
PROOF OF PROPOSITION 4

For conventional SIC, the decoding order is based on the magnitude of the $|h_{n,k}|^2$ which is noted by $\mathbf{Q}_n^{\text{COV}}$. Therefore, the outage probability error floor is given by

$$\mathbb{P}\left(R_{n,k}^{(\mathbf{Q}_n^{\text{COV}})} < R_k\right) \quad (42)$$

$$= \mathbb{P}\left(\frac{\eta_k P_{\text{BD}_k}|h_{n,k}|^2}{I_{\text{Intra},n}^{(\mathbf{Q}_n^{\text{COV}})}(k) + I_{\text{Inter}}(n) + \delta_n} < \gamma_k\right) \quad (43)$$

$$= \mathbb{P}\left(I_{\text{Intra},n}^{(\mathbf{Q}_n^{\text{COV}})}(k) > \frac{\eta_k P_{\text{BD}_k}|h_{n,k}|^2}{\gamma_k} - I_{\text{Inter}}(n) - \delta_n\right). \quad (44)$$

For the proposed decoding order scheme for SIC process, the outage probability error floor is given by

$$\mathbb{P}\left(R_{n,k}^{(\mathbf{Q}_n)} < R_k\right) \quad (45)$$

$$= \mathbb{P}\left(I_{\text{Intra},n}^{(\mathbf{Q}_n)}(k) > I_{\max,n}(k)\right) \quad (46)$$

$$= \mathbb{P}\left(I_{\text{Intra},n}^{(\mathbf{Q}_n)}(k) > \max\left\{0, \frac{\eta_k P_{\text{BD}_k}|h_{n,k}|^2}{\gamma_k} - I_{\text{Inter}}(n) - \delta_n\right\}\right). \quad (47)$$

When decoding the signal from BD_k, the upper bound of the intra-cell interference for BS_n is $\sum_{i=1,i\neq k}^{K} x_{n,i}\eta_i P_{\text{BD}_i}|h_{n,i}|^2$. If hybrid SIC is implemented, the decoding order is based on the magnitude of $I_{\max,n}(k)$, therefore, the upper bound of intra-cell interference is higher than that of conventional SIC, i.e., $I_{\text{Intra},n}^{(\mathbf{Q}_n)}(k) \geq I_{\text{Intra},n}^{(\mathbf{Q}_n^{\text{COV}})}(k)$. Therefore, $\mathbb{P}(R_{n,k}^{(\mathbf{Q}_n)} < R_k) \leq \mathbb{P}(R_{n,k}^{(\mathbf{Q}_n^{\text{COV}})} < R_k)$, which indicates that the implementation of hybrid SIC can better deal with the outage performance compared with conventional SIC.

REFERENCES

[1] X. Xie and Z. Ding, "Backscatter-assisted non-orthogonal multiple access network for next generation communication," *IET Signal Process.*, vol. 17, no. 4, Apr. 2023, Art. no. e12211.

[2] X. Xie, S. Jiao, K. Wang, and Z. Ding, "BAC-NOMA for secondary transmission," *IEEE Commun. Lett.*, vol. 27, no. 9, pp. 2481–2485, Sep. 2023.

[3] Y. Ye, L. Shi, X. Chu, D. Li, and G. Lu, "Delay minimization in wireless powered mobile edge computing with hybrid BackCom and AT," *IEEE Wireless Commun. Lett.*, vol. 10, no. 7, pp. 1532–1536, Jul. 2021.

[4] Z. Ding and H. V. Poor, "Advantages of NOMA for multi-user BackCom networks," *IEEE Commun. Lett.*, vol. 25, no. 10, pp. 3408–3412, Oct. 2021.

[5] Y. Liu, J. Ma, Y. Ye, X. Li, and Y. Zhao, "Outage performance of BackCom systems with multiple self-powered tags under channel estimation error," *IEEE Commun. Lett.*, vol. 26, no. 7, pp. 1548–1552, Jul. 2022.

[6] Y. Lin, K. Wang, and Z. Ding, "Unsupervised machine learning-based user clustering in THz-NOMA systems," *IEEE Wireless Commun. Lett.*, vol. 12, no. 7, pp. 1130–1134, Jul. 2023.

[7] C. Zhao, Y. Liu, Y. Cai, M. Zhao, and Z. Ding, "Non-orthogonal multiple access for UAV-aided heterogeneous networks: A stochastic geometry model," *IEEE Trans. Veh. Technol.*, vol. 72, no. 1, pp. 940–956, Jan. 2023.

[8] A. Huang, L. Guo, X. Mu, C. Dong, and Y. Liu, "Coexisting passive RIS and active relay-assisted NOMA systems," *IEEE Trans. Wireless Commun.*, vol. 22, no. 3, pp. 1948–1963, Mar. 2023.

[9] J. Xu, X. Mu, J. T. Zhou, and Y. Liu, "Simultaneously transmitting and reflecting (STAR)-RISs: Are they applicable to dual-sided incidence?" *IEEE Wireless Commun. Lett.*, vol. 12, no. 1, pp. 129–133, Jan. 2023.

[10] K. Wang, F. Fang, D. B. D. Costa, and Z. Ding, "Sub-channel scheduling, task assignment, and power allocation for OMA-based and NOMA-based MEC systems," *IEEE Trans. Commun.*, vol. 69, no. 4, pp. 2692–2708, Apr. 2021.

[11] C. Guo, J. Xin, L. Zhao, and X. Chu, "Performance analysis of cooperative NOMA with energy harvesting in multi-cell networks," *China Commun.*, vol. 16, no. 11, pp. 120–129, Nov. 2019.

[12] Y. Sun and X. Dai, "Stochastic geometry based modeling and analysis on network NOMA in vehicular networks," in *Proc. IEEE Int. Conf. Commun. Workshops (ICC Workshops)*, 2020, pp. 1–6.

[13] T. Wang, F. Fang, and Z. Ding, "An SCA and relaxation based energy efficiency optimization for multi-user RIS-assisted NOMA networks," *IEEE Trans. Veh. Technol.*, vol. 71, no. 6, pp. 6843–6847, Jun. 2022.

[14] J. Guo, X. Zhou, S. Durrani, and H. Yanikomeroglu, "Backscatter communications with NOMA (invited paper)," in *Proc. 15th Int. Symp. Wireless Commun. Syst. (ISWCS)*, 2018, pp. 1–5.
[15] Z. Ding and H. V. Poor, "On the application of BAC-NOMA to 6G umMTC," *IEEE Commun. Lett.*, vol. 25, no. 8, pp. 2678–2682, Aug. 2021.
[16] D. Lin, K. Cumanan, and Z. Ding, "Beamforming design for BackCom assisted NOMA systems," *IEEE Wireless Commun. Lett.*, vol. 12, no. 9, pp. 1494–1498, Sep. 2023.
[17] D. Lin, T. Wang, K. Wang, and Z. Ding, "EE Maximization in BackCom NOMA system: Dinkelbach and SCA approaches," *IET Signal Process.*, 2023, preprint.
[18] Y. Xu, S. Jiang, Q. Xue, X. Li, and C. Yuen, "Throughput maximization for NOMA-based cognitive backscatter communication networks with imperfect CSI," *IEEE Internet Things J.*, vol. 10, no. 22, pp. 19595–19606, Nov. 2023.
[19] Y. Xu et al., "Robust resource allocation for wireless-powered backscatter communication systems with NOMA," *IEEE Trans. Veh. Technol.*, vol. 72, no. 9, pp. 12288–12299, Sep. 2023.
[20] T. T. Hoang, H. D. Le, X. L. Nguyen, and C. T. Nguyen, "On the design of NOMA-enhanced backscatter communication systems," *IEEE Access*, vol. 11, pp. 44759–44771, 2023.
[21] D. Galappaththige, F. Rezaei, C. Tellambura, and S. Herath, "Beamforming designs for enabling symbiotic BackCom multiple access under imperfect CSI," *IEEE Access*, vol. 11, pp. 89986–90005, 2023.
[22] W.-G. Zhou, "Max-min throughput in hybrid of wireless powered NOMA and backscatter communications," *IEEE Access*, vol. 8, pp. 204459–204470, 2020.
[23] F. M. Caceres, K. Sithamparanathan, and S. Sun, "Theoretical analysis of hybrid SIC success probability under rayleigh channel for uplink CR-NOMA," *IEEE Trans. Veh. Technol.*, vol. 71, no. 10, pp. 10584–10599, Oct. 2022.
[24] K. Wang, H. Li, Z. Ding, and P. Xiao, "Reinforcement learning based latency minimization in secure NOMA-MEC systems with hybrid SIC," *IEEE Trans. Wireless Commun.*, vol. 22, no. 1, pp. 408–422, Jan. 2023.
[25] Z. Ding, R. Schober, and H. V. Poor, "Unveiling the importance of SIC in NOMA systems—Part-1: State of the art and recent findings," *IEEE Commun. Lett.*, vol. 24, no. 11, pp. 2373–2377, Nov. 2020.
[26] Z. Ding, R. Schober, and H. V. Poor, "Unveiling the importance of SIC in NOMA systems—Part-II: New results and future directions," *IEEE Commun. Lett.*, vol. 24, no. 11, pp. 2378–2382, Nov. 2020.
[27] M. Al-Imari, P. Xiao, M. A. Imran, and R. Tafazolli, "Uplink non-orthogonal multiple access for 5G wireless networks," in *Proc. 11th Int. Symp. Wireless Commun. Syst. (ISWCS)*, 2014, pp. 781–785.
[28] K. Wang, Y. Liu, Z. Ding, A. Nallanathan, and M. Peng, "User association and power allocation for multi-cell non-orthogonal multiple access networks," *IEEE Trans. Wireless Commun.*, vol. 18, no. 11, pp. 5284–5298, Nov. 2019.
[29] A. Rezaei, P. Azmi, N. M. Yamchi, M. R. Javan, and H. Yanikomeroglu, "Robust resource allocation for cooperative MISO-NOMA-based heterogeneous networks," *IEEE Trans. Commun.*, vol. 69, no. 6, pp. 3864–3878, Jun. 2021.
[30] K. Shen and W. Yu, "Fractional programming for communication systems—Part-I: Power control and beamforming," *IEEE Trans. Signal Process.*, vol. 66, no. 10, pp. 2616–2630, May 2018.
[31] K. Shen and W. Yu, "Fractional programming for communication systems—Part-II: Uplink scheduling via matching," *IEEE Trans. Signal Process.*, vol. 66, no. 10, pp. 2631–2644, May 2018.
[32] S. Seidel and T. Rappaport, "914 MHz path loss prediction models for indoor wireless communications in multifloored buildings," *IEEE Trans. Antennas Propag.*, vol. 40, no. 2, pp. 207–217, Feb. 1992.